Neuro-Oncology
22(3), 423–432, 2020 | doi:10.1093/neuonc/noz171 | Advance Access date 9 September 2019

High-resolution MRI demonstrates that more than 90% of small intracranial melanoma metastases develop in close relationship to the leptomeninges

Arian Lasocki, Chloe Khoo, Peter K. H. Lau, David L. Kok, and Grant A. McArthur

Department of Cancer Imaging, Peter MacCallum Cancer Centre, Melbourne, Victoria, Australia (A.L.); Sir Peter MacCallum Department of Oncology, The University of Melbourne, Parkville, Victoria, Australia (A.L., G.A.M.); Department of Medical Oncology, Peter MacCallum Cancer Centre, Melbourne, Victoria, Australia (C.K., P.K.H.L., G.A.M.); Department of Radiation Oncology, Peter MacCallum Cancer Centre, Melbourne, Victoria, Australia (D.L.K.); Melbourne Medical School, The University of Melbourne, Parkville, Victoria, Australia (D.L.K.)

Corresponding Author: Dr Arian Lasocki, Department of Cancer Imaging, Peter MacCallum Cancer Centre, Grattan St, Melbourne, Victoria 3000, Australia (arian.lasocki@petermac.org).

Abstract

Background. Despite classic teaching that intracranial metastases typically arise at the gray–white matter junction, small intracranial melanoma metastases (IMM) are frequently observed at the interface between the cortex and leptomeninges (ie, "corticomeningeal interface"), suggesting possible leptomeningeal origin.

Methods. MRI brain examinations of melanoma patients treated at a specialist oncology center from July 2015 to June 2017 were retrospectively reviewed. The MRI examination on which IMM were first visible was identified, utilizing 1 mm volumetric postcontrast imaging prior to local therapy. Individual metastases (up to 10 per patient) were assessed for the presence of leptomeningeal contact, as well as their number, size, and morphology. Lesions ≥10 mm in long axis were excluded, in order to examine early metastatic disease.

Results. Seventy-five patients had evidence of IMM. Fifteen patients had only lesion(s) measuring ≥10 mm at diagnosis, leaving 60 patients. One hundred ninety-two individual metastases were examined (median 2 per patient; interquartile range, 1–4), 174 (91%) demonstrating leptomeningeal contact. A nodular morphology was observed in 154 of 192 (82%), 32 (17%) were ovoid but elongated along the cortex, and 6 (3%) were linear. Only 3 patients (5%) also exhibited a "classic" linear leptomeningeal disease appearance.

Conclusions. Most IMM measuring between 2 and 9 mm in diameter are corticomeningeal nodules. These data raise the hypothesis that deeper parenchymal extension of IMM occurs secondarily. If the leptomeninges provide a preferential site for establishment of IMM, further investigation of the underlying biology of this phenomenon may provide opportunities for novel therapeutic strategies for patients with IMM.

Key Points

1. Most small IMM develop at the corticomeningeal interface, rather than the gray–white junction.
2. This suggests that the pia mater provides a preferential site for establishment of IMM.
3. Deeper brain parenchymal extension may occur secondarily.

Brain metastases are a frequent complication in patients with advanced melanoma, and represent a significant cause of morbidity and mortality. Historically, patients with melanoma brain metastases had a median overall survival (OS) of 4 to 6 months, or less than 2 months if leptomeningeal disease was present.[1] Modern therapies such as

Importance of the Study

Most IMM measuring between 2 and 9 mm originate in close relationship to the leptomeninges, most commonly at the interface between the pia and the cortex, but also along the ventricular system and in typical locations for perivascular spaces. This is a subtle but important difference compared with conventional wisdom, namely that intracranial metastases usually develop at the gray–white matter junction. These data raise the hypothesis that the leptomeninges, in particular the pia mater, provide a preferential site for establishment of IMM, with deeper parenchymal extension occurring secondarily. Further investigation of the underlying biology of this phenomenon may provide opportunities for novel therapeutic strategies for patients with IMM.

immune checkpoint inhibitors and BRAF-targeted therapy have changed the overall landscape of metastatic melanoma, resulting in an unprecedented gain in survival, with a 5-year OS of 34% seen with single agent anti–programmed cell death protein 1 (PD-1),[2] a 4-year OS of 43% with combined anti–cytotoxic T-lymphocyte-associated protein 4 and anti–PD-1,[3] and a 4-year OS of 30% with BRAF and MEK inhibitors using dabrafenib and trametinib.[4] Although intracranial melanoma metastases (IMM) do respond to these novel therapies in many cases,[5–8] intracranial metastatic disease remains a major cause of death, with recent series demonstrating an OS of 7–12 months in patients with IMM, even in the era of these novel therapies.[9,10]

The pathogenesis of IMM has been studied in a variety of mouse models. The pattern of IMM varies depending on the cell line utilized, with certain melanoma cell lines having a distinct preference for meningeal metastases.[11–17] Schackert et al found that, after injecting melanoma cells into the internal carotid arteries of nude mice, cell lines developed from subcutaneous and lymph node metastases grew more frequently in the meninges and ventricles, while lines developed from parenchymal brain metastases showed a preference for brain parenchymal growth.[16] Similar findings were demonstrated by Fidler et al.[12] Küsters et al also demonstrated substantial differences in the pattern of metastatic disease between cell lines.[13] Of the 4 cell lines injected, 2 cells lines produced meningeal metastases, frequently with secondary brain parenchymal involvement, while the other 2 showed primary brain parenchymal involvement.[13] Supporting the findings by Schackert et al, one of the 2 cells associated with a preference for primary brain parenchymal involvement was derived from a brain metastasis.[13]

Subsequent research has suggested that expression of transforming growth factor β2 (TGF-β2) is necessary for the establishment of brain metastases in the brain parenchyma.[18] The murine B16 melanoma cells studied had a low expression of this factor and demonstrated intracranial metastases only to the leptomeninges and ventricles. Transfection of the TGF-β2 gene into B16 cells resulted, however, in the production of microscopic metastatic lesions in the brain parenchyma, without a decrease in metastases to the leptomeninges or ventricles.[18] More recently, Simonsen et al investigated the pattern of intracranial metastatic disease from 4 different melanoma cell lines which had previously been shown to differ substantially in their properties, using both direct intracerebral and intra-arterial injection.[14] Even with direct intracerebral injection, macroscopic tumor growth in the brain parenchyma was observed in fewer than 5% of mice, whereas macroscopic tumor growth was visible in the meninges in a majority of mice injected with all 4 cell lines.[14] Intra-arterial injection resulted in the metastases to the meninges and ventricles, though the lesions were smaller due to extracranial metastatic disease limiting survival.[14] For 3 of 4 cell lines, meningeal involvement was followed by secondary involvement of the brain parenchyma.[14]

There are several difficulties with translating mouse models to human disease, and given that brain parenchymal involvement seems to predominate in humans, it is unclear how relevant the above results are.[19] For example, the manner in which brain metastases are reproduced in most mouse models, such as single-dose direct intracarotid or intracerebral injection, does not reflect the real-life setting, when the release of tumor cells is likely to be more gradual and requires invasion, intravasation, and extravasation.[19] The pattern of metastatic disease is also clearly influenced by the melanoma cell line utilized, and the variability in melanoma cell lines studied indicates uncertainly as to the optimal model. Indeed, no single model can be expected to replicate the behavior of all human melanomas given their heterogeneity. Thus, the underlying mechanisms by which melanoma cells enter the central nervous system (CNS) remain uncertain.

Classic radiological teaching is that intracranial metastases most commonly arise at the gray–white matter junction, related to branching and tapering of vessels at the transition from the abundant vessels in the cortical gray matter to the relatively sparse vasculature of white matter.[20] With the benefit of modern MRI, however, small IMM are frequently observed at the interface between the cortex and leptomeninges ("corticomeningeal interface"), suggesting possible leptomeningeal origin. As IMM enlarge, the greater volume of parenchymal involvement—often including the cortex, gray–white matter junction, and subcortical white matter—makes it more difficult to determine the site of origin. We sought, therefore, to systematically investigate the development of small IMM utilizing modern, fine-slice MRI.

Materials and Methods

This was a retrospective, single-institution study undertaken at the Peter MacCallum Cancer Centre, a specialist

oncology center. The study was approved by the institutional human research ethics committee (project number 18/90R).

Patient Cohort

Imaging reports for all patients who attended the Skin and Melanoma Medical Oncology outpatient clinic between July 2015 and June 2017 were reviewed. Patients were included in the study if their first diagnosis of IMM was detected on brain MRI examinations performed in our radiology department, prior to any local therapy (surgical resection, stereotactic radiosurgery, and/or whole-brain radiotherapy). All examinations were performed on a 3-Tesla MRI (Magnetom Trio or Magnetom Skyra, Siemens), with a standardized protocol utilizing 1 mm volumetric pre- and postcontrast imaging (MPRAGE [magnetization prepared rapid acquisition gradient echo]) with fat suppression. The protocol also included at least axial T2-weighted imaging, axial fluid-attenuated inversion recovery, and susceptibility weighted imaging. Patients were excluded if they fulfilled any of the following criteria: diagnosis other than melanoma, insufficient patient information, pre- and postcontrast MRI from our institution not available at the time of diagnosis of IMM, no IMM identified. Patients with primary meningeal melanoma or perineural pattern spread only were also excluded. The exclusions are presented in Fig. 1. Background information including age, sex, BRAF status, and prior treatment was also collected.

Radiological Assessments

MR images of patients fulfilling the eligibility criteria were reviewed by a single experienced neuroradiologist to confirm a confident diagnosis of IMM and determine the MRI examination on which the IMM were first visible. Individual metastases were assessed, excluding lesions ≥10 mm in long axis, in order to examine early metastatic disease. To allow a confident diagnosis of IMM, lesions were only included if they measured at least 2 × 2 mm if nodular or at least 3 mm in long axis if linear. Up to 10 metastases were assessed per patient; if more than 10 IMM were present, the largest 10 lesions were chosen as per the aforementioned criteria. The following features were assessed for each metastasis: lobar location, long and short axis diameters, and morphology (nodular, ovoid and elongated along the cortex, or linear, including curvilinear). The location with respect to the leptomeninges was examined: corticomeningeal, including at the periphery of the brain, within a cerebral sulcus or along a cerebellar folium; contacting the ependymal surface of the ventricular system; or no meningeal contact. Representative images are provided in Fig. 2. Assessment was predominantly performed in the axial plane, but other planes and/or other sequences were reviewed where appropriate in order to provide the most accurate characterization—examples are provided in Fig. 3. The presence of leptomeningeal disease within the cerebral sulci and/or along cranial nerves or the ependyma was also recorded.

Results

Between July 2015 and June 2017, seven hundred thirty-six patients had a total of 3446 outpatient presentations to the Skin and Melanoma Medical Oncology clinic, of whom 75 patients had a first diagnosis of IMM on pre- and postcontrast MRI performed at our institution prior to any local treatment. Fifteen patients had only intracranial lesion(s) measuring ≥10 mm at diagnosis, resulting in 60 eligible patients for the final analysis (Fig. 1). Thirty-nine patients (65%) were male, and the median age at the time of IMM diagnosis was 60 years (range, 23–89 y). A BRAF V600 mutation was present in 38 patients (63%); 29 patients (48%) had not received any systemic therapy prior to the development of IMM; the remainder had most commonly received combination dabrafenib/trametinib and/or immunotherapy. The above background data are summarized in Table 1.

A total of 192 individual IMM were examined, with a median of 2 metastases measuring 2–9 mm per patient (interquartile range, 1–4)—the frequency distribution of metastases per patient is presented in Table 2. Most (n = 151) IMM were supratentorial in location (frontal, n = 61; temporal, n = 45; parietal, n = 25; occipital, n = 16; insular, n = 4), while most infratentorial lesions were cerebellar (20 of 23). One hundred sixty-nine (88%) IMM were located at the corticomeningeal interface, most commonly nodular in morphology (n = 132) or elongated along the cortex (n = 32), and least frequently linear (n = 5). A further 5 lesions (3%) demonstrated ependymal contact, 4 nodular and 1 linear. The remaining 18 metastases without apparent meningeal contact all had a nodular morphology; 11 occurred in the basal ganglia region, including the lentiform nuclei (n = 6), thalami (n = 3), caudate nuclei (n = 1), and external capsules (n = 1), while the remaining 7 were located in the frontal lobes (n = 5), temporal lobes (n = 1), and midbrain (n = 1). The distribution of IMM, in terms of both their anatomical location and meningeal contact, was similar in patients with both a BRAF V600 mutation (126 IMM in 38 patients) and those without a BRAF V600 mutation (66 IMM in 22 patients, including 1 patient with a BRAF G466V mutation)—these data are also included in Table 2. In addition, the proportion of lesions with meningeal contact was similar in both treatment-naïve patients (85 of 93 IMM, or 91%) and in those who had had previous systemic treatment (89 of 99 IMM, or 90%).

Seventeen patients had a total of 20 cerebellar IMM, with 3 of these patients having 2 cerebellar IMM. Of these 17 patients, 12 had synchronous IMM supratentorially, with the remaining 5 patients having disease isolated to the cerebellum (4 patients with a solitary lesion, 1 with 2 lesions). Three individual ependymal IMM occurred in a patient who largely had ependymal disease (with only one further lesion ≥10 mm in size), both including these 3 discrete lesions and more extensive linear ependymal disease. Two patients had one ependymal lesion each, one with an ependymal lesion and three 2–9 mm corticomeningeal lesions, the final patient with a total of 9 IMM in a mixture of locations (corticomeningeal, basal ganglia region, and lobar without meningeal contact). The midbrain lesion was

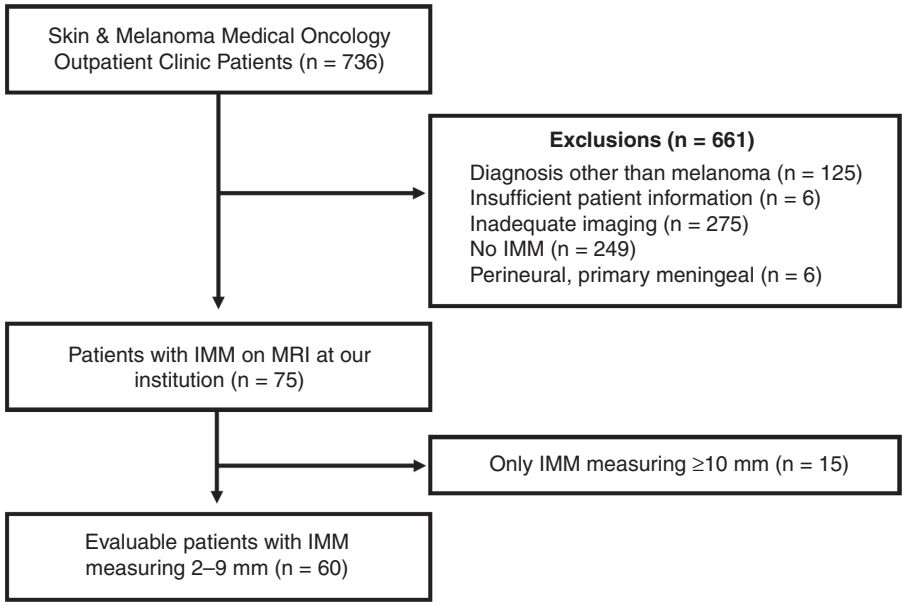

Fig. 1 Study flow chart diagram of included patients with IMM.

solitary. There were only 6 non-corticomeningeal lobar IMM, occurring in 4 patients (2 patients having 2 such lesions). Three of these 4 patients had a high number of IMM (a total of 7, 9, and ≥10 metastases, respectively); for the fourth patient, this lesion was solitary. Only 3 patients (5%) also exhibited linear leptomeningeal disease either along cranial nerves ($n = 2$) or within the cerebral sulci ($n = 1$).

Discussion

The majority of the small IMM in our cohort were located at the corticomeningeal interface. The leptomeninges consist of 2 layers, the pia mater and the arachnoid, with the subarachnoid space in between the 2 layers.[21,22] The pia mater is intimately attached to the brain, extending into the sulci, while the arachnoid is closely applied to the inner surface of the dura.[22] The corticomeningeal interface thus corresponds to the pia mater rather than the arachnoid. The intimate relationship of the pia mater to the cortex accounts for the appearance of pial metastatic disease involving, and at times extending along, the cortex. Of the remaining metastases, a substantial number occurred in the basal ganglia region, a typical location for perivascular spaces. Leptomeningeal layers continuous with the pia mater extend around arteries within perivascular spaces.[23] Perivascular space involvement in leptomeningeal metastatic disease has been described both in mouse models[14,24] and at human autopsy,[25] and given that most other metastases were corticomeningeal (and likely pial), we suggest that the presence of pia mater within perivascular spaces may account for the higher frequency of basal ganglia metastases than would be expected for the anatomical size of this region. A single metastasis developed in the midbrain, and this is also a common location for perivascular spaces.[26] A few metastases were also demonstrated at the margin of the ventricular system. The ependymal lining of the ventricular system is intimately linked to the choroid plexus, which consists of a rich network of blood vessels of the pia mater.[21] Coexistence of meningeal and ventricular metastases has also been shown in mouse models.[13–16]

These 3 groups (corticomeningeal interface, in locations typical for perivascular spaces, and abutting the ventricular system) together accounted for 97% of all IMM studied in our series. The presence of the pia mater is common to all 3 sites, raising the hypothesis that the pia provides a preferential portal of entry for melanoma cells. Of note, the high incidence of meningeal contact was observed for patients both with and without a BRAF V600 mutation, as well as patients with and without prior systemic treatment. Thus, this portal does not appear to be significantly affected by BRAF status or prior systemic treatment.

Lobar, non-corticomeningeal IMM made up a small minority (3%) of the overall metastases, with a total of 6 lesions in 4 patients (2 patients with 2 such lesions). Of note, 3 of these 4 patients had a high number (within the top quartile) of IMM, though the small number of non-corticomeningeal lobar lesions limits statistical comparison. Based on the findings by Schackert et al described below, there is the potential that these spread from other intracranial metastases which had extended further into the parenchyma.

Classic radiological teaching is that intracranial metastases from solid organ metastases usually arise in the parenchyma, at the gray–white matter junction.[20] Prior research, however, may have been inherently biased by

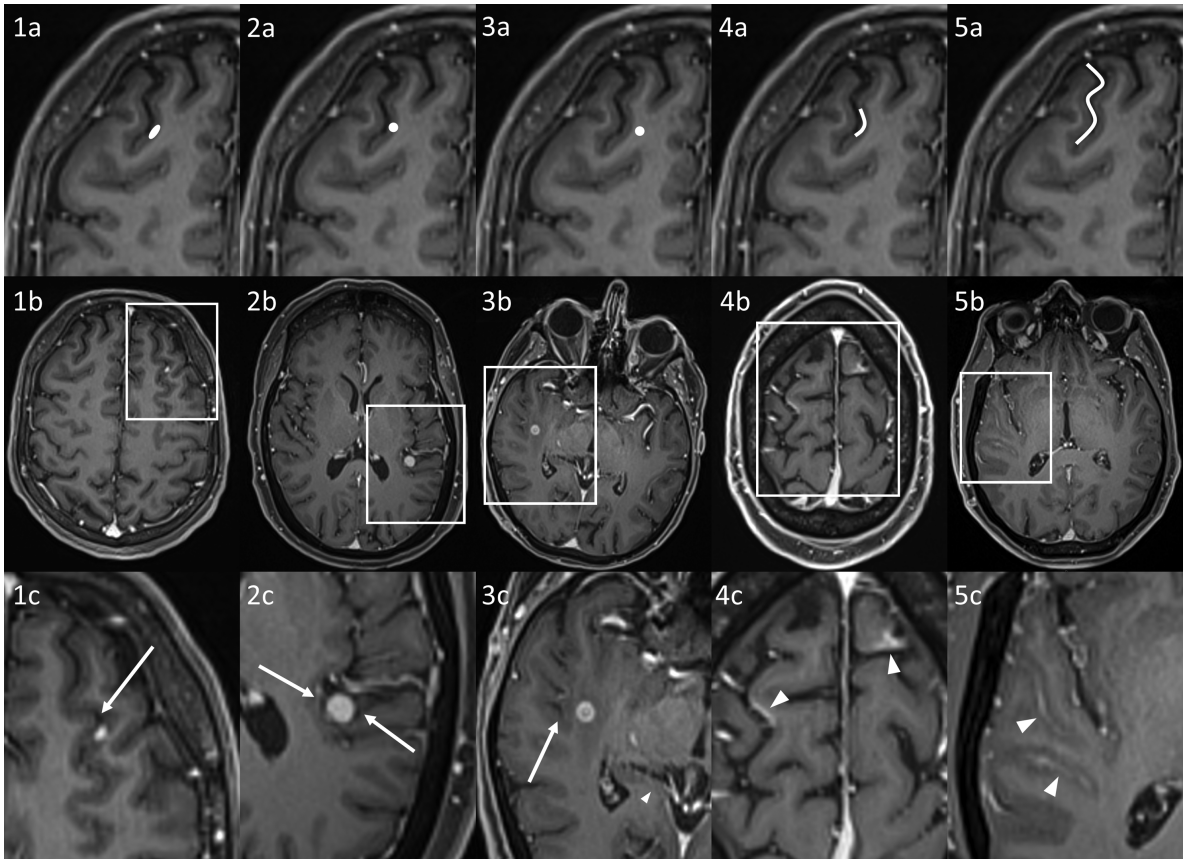

Fig. 2 Examples of different appearances of intracranial metastatic disease on postcontrast T1-weighted imaging, including diagrammatic representations (top row, a), patient examples (middle row, b) and zoomed panels (bottom row, c). 1a–c: elongated IMM involving the cortex and corticomeningeal interface, with broad pial contact. The IM metastasis involves the gray matter (dark gray), preserving the CSF (black, arrow). 2a–c: nodular IMM involving the cortex and corticomeningeal interface, also having broad pial contact (arrows), but not specifically elongated along the corticomeningeal interface. 3a–c: IMM at the gray–white matter junction, without meningeal contact (CSF shown by the arrow). 4a–c: curvilinear IMM (arrowheads) along the corticomeningeal interface, without significant effacement of the CSF in the subarachnoid space (black). 5a–c: "classic" leptomeningeal metastatic disease involving the subarachnoid space (arrowheads); in contrast to example 4, the CSF in the subarachnoid space is effaced.

grouping solid organ metastases together. For example, in their study assessing the pattern of intracranial metastases in 105 patients, Hwang and colleagues found that the majority developed at the gray–white matter junction.[27] Only 3 patients in their series had melanoma, however, with the majority having a lung primary.[27] Similarly, in a recent study assessing the location of 150 metastases in 28 patients, all patients had either a lung or breast primary.[28] The proclivity of cells from a particular cancer type to preferentially metastasize to certain anatomical locations is well established.[29] This is equally true regarding the distribution of metastases to the brain—for example, some primaries have a greater tendency to posterior fossa involvement.[30] Given the fundamental differences in the sites of origin of metastases grouped together as "solid organ malignancies," and in the genetic pathways involved in their carcinogenesis, it is not unexpected that the biological mechanisms of intracranial metastatic disease—and therefore the relative incidence of leptomeningeal involvement—would vary between primaries. Indeed, differences in the spatial distribution of intracranial metastases from lung cancer have been shown based on histological subtype and epidermal growth factor receptor mutation status.[31] As such, the pattern of intracranial metastatic disease from a limited number of primaries cannot necessarily be extrapolated to metastases from other primary sites, such as melanoma.

There has been some skepticism in the literature about the validity of mouse models showing a preference for meningeal metastases as a surrogate of human disease, citing differences to autopsy results.[19,32] The autopsy data are limited and conflicting, however.[25,32,33] In the cited series by Patel et al, melanoma metastases were twice as common in the brain as in the meninges, but brain and meningeal involvement were separated,[32] thus it is unclear how often both were involved. In stark contrast, de la Monte et al found that the gray matter and leptomeninges were the most common sites of intracranial metastases,

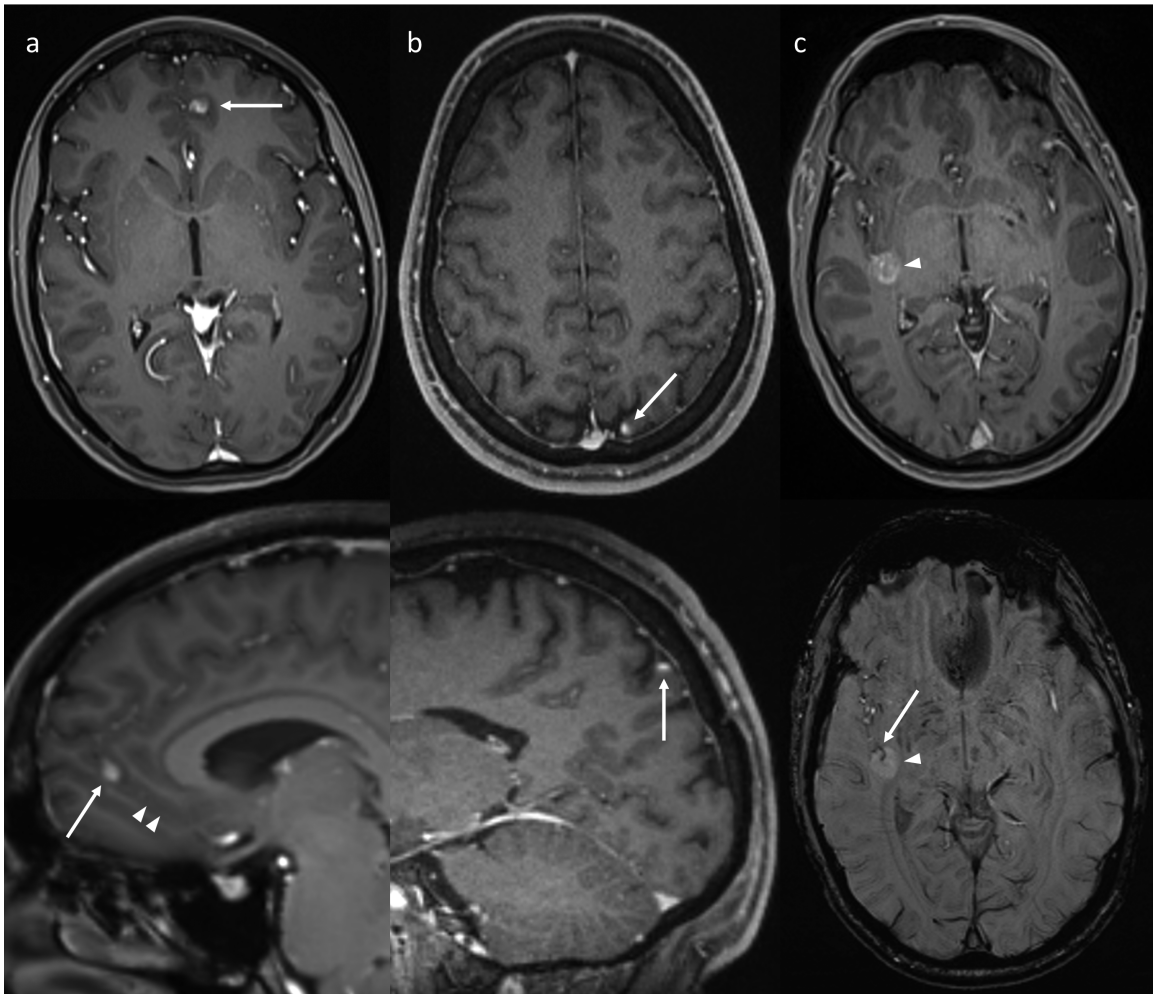

Fig. 3 Examples of using other planes and sequences (bottom images) to improve characterization of IMM identified on axial post-contrast imaging (top images). (a) The sagittal reconstruction (bottom) better demonstrates an elongated morphology of the IMM (arrows) being oriented along a sulcus (arrowheads). (b) The sagittal plane (bottom) helps confirm that the IM metastasis (arrows) is oriented along the corticomeningeal interface. (c) Susceptibility weighted imaging (bottom) shows a vessel within the central sulcus (arrow) passing into the middle of the IMM (arrowhead), showing that the IM metastasis surrounds the central sulcus. This relationship is not as well appreciated on the postcontrast image (top).

occurring in 88% and 63% of cases, respectively.[25] These 2 sites strongly correlated with each other, which was attributed by the authors to direct extension.[25] An autopsy study by Amer et al yielded similar results.[33] Meningeal metastases were found in 70% of patients with CNS metastases, often occurring in conjunction with brain parenchymal metastases, and the authors felt that many further cases of meningeal disease had been missed, related to sampling error.[33]

Autopsy studies are inevitably biased toward patients with much bulkier and more advanced disease, due to intracranial metastatic disease being a frequent cause of death.[32] With mouse models showing that IMM with brain parenchymal involvement have a greater propensity to in turn metastasize directly to the brain,[12,13,16] the proportion of parenchymal compared with meningeal metastases should increase as the intracranial disease progresses. Histological data from neurosurgical resection has similar limitations. Currently, most small IMM are treated with medical therapy and/or radiotherapy (either stereotactic radiosurgery or whole-brain radiotherapy depending on the size and number of lesions), while neurosurgical resection is generally reserved for metastases which either are larger at presentation (providing a poor indicator of the site at which melanoma cells initially enter the CNS) or have progressed or recurred after other treatments (which could affect the subsequent pattern of growth).

Given these difficulties, MRI has significant advantages for examining the initial development and subsequent evolution of IMM. Nevertheless, some autopsy data already exist to support our hypothesis,[25,33] and the hypothesis is further supported by some mouse studies which

Table 1 Background patient information and number of patients with a given number of IMM

	n (%)
Sex	
Male	39 (65)
Female	21 (35)
Age	
<50	19 (32)
50–59	11 (18)
60–69	17 (28)
≥70	13 (22)
BRAF status	
BRAF V600 mutation	38 (63)
V600E	29
V600K	9
No BRAF V600 mutation	22 (37)
BRAF wild-type	21
BRAF G466V mutation	1
Previous treatment	
None	29 (48)
Single line of treatment	19 (32)
BRAFi ± MEKi*	13
Immunotherapy	5
Interferon	1
2 or more lines	12 (20)
Metastases per patient**	
1	26 (43)
2–4	21 (35)
5–9	7 (12)
≥10	6 (10)

*BRAF inhibitor ± MEK inhibitor.
**Including only 2–9 mm metastases.

demonstrated that some melanoma cells have a predilection for the meninges.[11–17] Importantly, our study is, to our knowledge, the first to provide more compelling evidence that similar mechanisms may also occur in humans.

The classic imaging description of leptomeningeal metastatic disease is abnormal enhancement within the cerebral sulci, cisterns, and cerebellar folia,[20] corresponding to the location of the subarachnoid space. This appearance differs from the corticomeningeal interface involvement we have described, in which the cerebrospinal fluid within the sulci is generally not effaced, suggesting minimal extension into the subarachnoid space. The high frequency of metastases contacting the pia mater suggests that this particular layer of the leptomeninges provides a preferential portal of entry for melanoma cells into the CNS, with parenchymal involvement occurring secondarily. This is in line with mouse models,[13,14] but our finding that this appears to also be the dominant mechanism in humans is novel. While this differs significantly from conventional wisdom, it is not entirely surprising, as imaging technology has improved dramatically. The superiority of MRI over CT is well established, and the increased utilization of 3-Tesla MRI scanners and volumetric imaging now allows the detection and characterization (both anatomical and morphological) of metastases as small as 1–2 mm. Thus, up until recently, small corticomeningeal interface metastases would not have been identified until they enlarged to a size that their site of origin could no longer be distinguished. To our knowledge, there is no uniform definition of leptomeningeal metastatic disease, despite this often being an important variable in clinical studies. We recommend, therefore, that leptomeningeal disease be specifically separated between that involving the subarachnoid space and that confined to a pial or corticomeningeal interface location, with the potential for further subclassification based on morphology (nodular or curvilinear).

Of note, some patients with corticomeningeal interface metastases were involved in clinical trials which excluded patients with leptomeningeal metastatic disease. Indeed, given our findings of a very high incidence of corticomeningeal metastases, we expect that this would also be the case for contemporary trial patients at other institutions. This is not surprising, as the presence of leptomeningeal contact (and suspected origin) is easily missed if this relationship is not appreciated or assessed, especially if high resolution imaging was not performed. We have not formally analyzed response rates for patients with corticomeningeal interface IMM given that no standardized response criteria exist for small IMM. Nonetheless, we suggest that response to therapy would be similar or identical to the broader cohort of intracranial metastatic disease based on patterns of progression. Indeed, our data provide reassurance that data from trials thought to exclude leptomeningeal metastases can be extrapolated to patients in whom pial contact is identified. Some IMM have a propensity to extend along the corticomeningeal interface, as demonstrated by the lesions with a curvilinear morphology, suggesting that the pial margins may be a site at risk of recurrence after stereotactic radiosurgery. Given that we have only examined IMM prior to local treatment, however, we cannot determine whether this should be taken into account when planning radiotherapy fields.

The focus on small metastases utilizing a standardized imaging protocol is a strength of our study. Although this decreases the number of IMM included in our study, it nevertheless remains a large cohort. We have also aimed to avoid selection bias by including all patients with appropriate imaging, which also overcomes the limitations afforded by the retrospective nature of the study. The single-reader nature is a potential limitation, though it does serve to remove the risk of interobserver variability. Pial and subarachnoid space involvement cannot be distinguished for the cerebellar lesions, due to the cerebellar folia being very thin. Similarly, there is the potential that some metastases (despite their small size) extended to the corticomeningeal interface after originating at the gray–white matter junction. Nevertheless, the majority of IMM had a convincing corticomeningeal interface origin. We are not able to provide the specific molecular mechanisms involved, but our findings will allow prior results

Table 2 Location of all IMM, stratified by morphology and presence of meningeal contact

Location	Total (%)	Morphology			Meningeal Contact	
		Nodular	Elongated	Linear	Yes	No
All IMM						
Supratentorial lobar	**151 (78.6)**	**119**	**28**	**4**	**145**	**6**
Frontal	61	49	11	1	56	5
Temporal	45	35	7	3	44	1
Parietal	25	20	5	0	25	0
Occipital	16	13	3	0	16	0
Insula	4	2	2	0	4	0
Basal ganglia region	**13 (6.8)**	**13**	**0**	**0**	**2**	**11**
Thalamus	5	5	0	0	2	3
Lentiform nucleus	6	6	0	0	0	6*
Caudate nucleus	1	1	0	0	0	1
External capsule	1	1	0	0	0	1*
Posterior fossa	**23 (12.0)**	**18**	**4**	**1**	**22**	**1**
Cerebellum	20	16	3	1	20	0
Midbrain	1	1	0	0	0	1
Pons	2	1	1	0	2	0
Ventricular	**5 (2.6)**	**4**	**0**	**1**	**5****	**0**
Total (%)	**192**	**154 (80.2%)**	**32 (16.7%)**	**6 (3.1%)**	**174 (90.6%)**	**18 (9.4%)**
BRAF V600 mutation						
Supratentorial lobar	**100 (79.3)**	**83**	**17**	**1**	**97**	**3**
Frontal	37	30	7	0	35	2
Temporal	32	28	3	1	31	1
Parietal	19	15	4	0	19	0
Occipital	9	7	2	0	9	0
Insula	3	2	1	0	3	0
Basal ganglia region	**8 (6.3)**	**8**	**0**	**0**	**0**	**8**
Thalamus	2	2	0	0	0	2
Lentiform nucleus	5	5	0	0	0	5*
Caudate nucleus	0	0	0	0	0	0
External capsule	1	1	0	0	0	1*
Posterior fossa	**14 (11.1)**	**11**	**2**	**1**	**13**	**1**
Cerebellum	12	10	1	1	12	0
Midbrain	1	1	0	0	0	1
Pons	1	0	1	0	1	0
Ventricular	**4 (3.2)**	**3**	**0**	**1**	**4****	**0**
Total (%)	**126**	**105 (83.3%)**	**19 (15.1%)**	**3 (2.4%)**	**114 (90.5%)**	**12 (9.5%)**
No BRAF V600 mutation						
Supratentorial lobar	**51 (77.3)**	**37**	**11**	**3**	**48**	**3**
Frontal	24	19	4	1	21	3
Temporal	13	7	4	2	13	0
Parietal	6	5	1	0	6	0
Occipital	7	6	1	0	7	0
Insula	1	0	1	0	1	0
Basal ganglia region	**5 (7.6)**	**5**	**0**	**0**	**2**	**3**
Thalamus	3	3	0	0	2	1

Table 2 Continued

Location	Total (%)	Morphology			Meningeal Contact	
		Nodular	Elongated	Linear	Yes	No
Lentiform nucleus	1	1	0	0	0	1*
Caudate nucleus	1	1	0	0	0	1
External capsule	0	0	0	0	0	0
Posterior fossa	**9 (13.6)**	**7**	**2**	**0**	**9**	**0**
Cerebellum	8	6	2	0	8	0
Midbrain	0	0	0	0	0	0
Pons	1	1	0	0	1	0
Ventricular	**1 (1.5)**	**1**	**0**	**0**	**1****	**0**
Total (%)	**66**	**50 (75.8%)**	**13 (19.7%)**	**3 (4.5%)**	**60 (90.9%)**	**6 (9.1%)**

Data have been provided for all IMM, as well as those in patients with a BRAF V600 mutation and those without.
*Based on the location, none would contact the meninges. **All considered to contact the meninges.

(which may not have been given sufficient credence) to be re-interpreted and future research to be better targeted.

Conclusions

Our findings indicate that most IMM measuring between 2 and 9 mm originate in close relationship to the leptomeninges, most commonly at the interface between the pia and the cortex, but also along the ventricular system and in typical locations for perivascular spaces. These data raise the hypothesis that the leptomeninges, in particular the pia mater, provide a preferential site for establishment of IMM, with deeper parenchymal extension occurring secondarily. Further investigation of the underlying biology of this phenomenon may provide opportunities for novel therapeutic strategies for patients with IMM. We also suggest that pial and subarachnoid space involvement be distinguished when diagnosing leptomeningeal metastatic disease.

Keywords

intracranial metastases | leptomeninges | magnetic resonance imaging | melanoma | pia mater.

Funding

None.

Conflict of interest statement. No conflicts of interest are reported.

Authorship statement. Study design: AL, CK, DK, GM. Data collection: AL, PKHL. Statistical analysis: AL. Manuscript preparation: AL, CK, DK, PKHL, GM. This study was presented at the 24th World Congress of Dermatology, June 2019, Milan, Italy.

References

1. Davies MA, Liu P, McIntyre S, et al. Prognostic factors for survival in melanoma patients with brain metastases. *Cancer.* 2011;117(8):1687–1696.
2. Hamid O, Robert C, Daud A, et al. Five-year survival outcomes for patients with advanced melanoma treated with pembrolizumab in KEYNOTE-001. *Ann Oncol.* 2019.
3. Hodi FS, Chiarion-Sileni V, Gonzalez R, et al. Nivolumab plus ipilimumab or nivolumab alone versus ipilimumab alone in advanced melanoma (CheckMate 067): 4-year outcomes of a multicentre, randomised, phase 3 trial. *Lancet Oncol.* 2018;19(11):1480–1492.
4. Long GV, Eroglu Z, Infante J, et al. Long-term outcomes in patients with BRAF V600-mutant metastatic melanoma who received dabrafenib combined with trametinib. *J Clin Oncol.* 2018;36(7):667–673.
5. Long GV, Atkinson V, Lo S, et al. Combination nivolumab and ipilimumab or nivolumab alone in melanoma brain metastases: a multicentre randomised phase 2 study. *Lancet Oncol.* 2018;19(5):672–681.
6. Long GV, Trefzer U, Davies MA, et al. Dabrafenib in patients with Val600Glu or Val600Lys BRAF-mutant melanoma metastatic to the brain (BREAK-MB): a multicentre, open-label, phase 2 trial. *Lancet Oncol.* 2012;13(11):1087–1095.
7. McArthur GA, Maio M, Arance A, et al. Vemurafenib in metastatic melanoma patients with brain metastases: an open-label, single-arm, phase 2, multicentre study. *Ann Oncol.* 2017;28(3):634–641.
8. Tawbi HA, Forsyth PA, Algazi A, et al. Combined nivolumab and ipilimumab in melanoma metastatic to the brain. *N Engl J Med.* 2018;379(8):722–730.

9. Tio M, Wang X, Carlino MS, et al. Survival and prognostic factors for patients with melanoma brain metastases in the era of modern systemic therapy. *Pigment Cell Melanoma Res.* 2018;31(4):509–515.
10. Vosoughi E, Lee JM, Miller JR, et al. Survival and clinical outcomes of patients with melanoma brain metastasis in the era of checkpoint inhibitors and targeted therapies. *BMC Cancer.* 2018;18(1):490.
11. Brunson KW, Beattie G, Nicolsin GL. Selection and altered properties of brain-colonising metastatic melanoma. *Nature.* 1978;272(5653):543–545.
12. Fidler IJ, Schackert G, Zhang RD, Radinsky R, Fujimaki T. The biology of melanoma brain metastasis. *Cancer Metastasis Rev.* 1999;18(3):387–400.
13. Küsters B, Westphal JR, Smits D, et al. The pattern of metastasis of human melanoma to the central nervous system is not influenced by integrin alpha(v)beta(3) expression. *Int J Cancer.* 2001;92(2):176–180.
14. Simonsen TG, Gaustad JV, Rofstad EK. Intertumor heterogeneity in vascularity and invasiveness of artificial melanoma brain metastases. *J Exp Clin Cancer Res.* 2015;34:150.
15. Schackert G, Fidler IJ. Site-specific metastasis of mouse melanomas and a fibrosarcoma in the brain or meninges of syngeneic animals. *Cancer Res.* 1988;48(12):3478–3484.
16. Schackert G, Price JE, Zhang RD, Bucana CD, Itoh K, Fidler IJ. Regional growth of different human melanomas as metastases in the brain of nude mice. *Am J Pathol.* 1990;136(1):95–102.
17. Alterman AL, Stackpole CW. B16 melanoma spontaneous brain metastasis: occurrence and development within leptomeninges blood vessels. *Clin Exp Metastasis.* 1989;7(1):15–23.
18. Zhang C, Zhang F, Tsan R, Fidler IJ. Transforming growth factor-beta2 is a molecular determinant for site-specific melanoma metastasis in the brain. *Cancer Res.* 2009;69(3):828–835.
19. Cruz-Muñoz W, Kerbel RS. Preclinical approaches to study the biology and treatment of brain metastases. *Semin Cancer Biol.* 2011;21(2):123–130.
20. Smirniotopoulos JG, Murphy FM, Rushing EJ, Rees JH, Schroeder JW. Patterns of contrast enhancement in the brain and meninges. *Radiographics.* 2007;27(2):525–551.
21. Noback CR, Strominger NL, Demarest RJ, Ruggiero DA. *The Human Nervous System: Structure and Function. 6th ed.* Totowa, NJ: Humana Press; 2005:89–99.
22. Meltzer CC, Fukui MB, Kanal E, Smirniotopoulos JG. MR imaging of the meninges. Part I. Normal anatomic features and nonneoplastic disease. *Radiology.* 1996;201(2):297–308.
23. Pollock H, Hutchings M, Weller RO, Zhang ET. Perivascular spaces in the basal ganglia of the human brain: their relationship to lacunes. *J Anat.* 1997;191 (Pt 3):337–346.
24. Brandsma D, Taphoorn MJ, Reijneveld JC, et al. MR imaging of mouse leptomeningeal metastases. *J Neurooncol.* 2004;68(2):123–130.
25. de la Monte SM, Moore GW, Hutchins GM. Patterned distribution of metastases from malignant melanoma in humans. *Cancer Res.* 1983; 43(7):3427–3433.
26. Saeki N, Sato M, Kubota M, et al. MR imaging of normal perivascular space expansion at midbrain. *AJNR Am J Neuroradiol.* 2005;26(3):566–571.
27. Hwang TL, Close TP, Grego JM, Brannon WL, Gonzales F. Predilection of brain metastasis in gray and white matter junction and vascular border zones. *Cancer.* 1996;77(8):1551–1555.
28. Yanagihara TK, Lee A, Wang TJC. Quantitative analysis of the spatial distribution of metastatic brain lesions. *Tomography.* 2017;3(1):16–22.
29. Saxena M, Christofori G. Rebuilding cancer metastasis in the mouse. *Mol Oncol.* 2013;7(2):283–296.
30. Delattre JY, Krol G, Thaler HT, Posner JB. Distribution of brain metastases. *Arch Neurol.* 1988;45(7):741–744.
31. Takano K, Kinoshita M, Takagaki M, et al. Different spatial distributions of brain metastases from lung cancer by histological subtype and mutation status of epidermal growth factor receptor. *Neuro Oncol.* 2016;18(5):716–724.
32. Patel JK, Didolkar MS, Pickren JW, Moore RH. Metastatic pattern of malignant melanoma. A study of 216 autopsy cases. *Am J Surg.* 1978;135(6):807–810.
33. Amer MH, Al-Sarraf M, Baker LH, Vaitkevicius VK. Malignant melanoma and central nervous system metastases: incidence, diagnosis, treatment and survival. *Cancer.* 1978;42(2):660–668.